ANALYSIS OF PRESSURE DROP IN ROD BUNDLES IN HEAVY LIQUID METAL

A. Batta, A. Class
Karlsruhe Institute of Technology, Germany
Hermann-von-Helmholtz-Platz 1,
76344 Eggenstein-Leopoldshafen, Germany
batta@kit.edu , class@ kit.edu

ABSTRACT

Early studies of the flow in rod bundles with spacer grids suggest that the pressure drop can be decomposed in contributions due to flow area variations by spacer grids and frictional losses along the rods. For these shape and frictional losses simple correlations based on theoretical and experimental data have been proposed. In the OECD benchmark study LACANNES it was observed that correlations could well describe the flow behaviour of the Heavy liquid metal (HLM) loop including a rod bundle with the exception of the core region, where different experts chose different pressure-loss correlations for the losses due to spacer grids. Here, RANS CFD simulations provided very good data compared to the experimental data. It was observed that the most commonly applied Rehme correlation underestimated the shape losses. In the MATTIS-H benchmark RANS CFD simulation of rod bundle flow with spacer grids was validated with experimental data based on water. Other studies have shown that very expensive LES simulation yields results of similar accuracy as RANS in the spacer grid region.

The expertise gained in from previous studies is applied to investigate a 19-pin HLM rod bundle experiment performed within the framework of the EU project THINS (thermalhydraulics of innovative nuclear systems). The experiment is performed at the Karlsruhe Liquid Metal Laboratory (KALLA) of Karlsruhe Institute of Technology (KIT). The tested bundle has characteristic dimensions close to the designed ADS European bundles for Gen-IV reactors. The current work summarize the results of hydraulic studies. The present numerical study investigates the pressure drop across the spacer grid. The proposed analysis methodology was verified based on experimental results. The verified computational method has been applied to test different flow cases which are formally identical when applying a correlation based on pressure loss coefficient and local blockage. The tested spacer is slightly non-symmetric in flow direction. Simulations showed around 14% difference in pressure losses for the forward and backward flow cases. The study shows that prediction of pressure drop across spacer grids by RANS-CFD using well resolved meshes in the spacer grid region yields more accurate results than any available correlation.

KEYWORDS
Liquid metal flow, grid spacer, pressure drop, CFD validation.

1. INTRODUCTION

Fuel assemblies are the most essential components in a reactor core and thus need accurate design. The study of its thermal hydraulic behavior is very eminent for safety features of the considered nuclear reactor. In some innovative nuclear reactor concepts, including accelerator driven systems (ADS) and the lead cooled fast reactor (LFR), heavy liquid metal is proposed to be used as coolant. Accordingly, the study of

thermal hydraulic behavior in these fuel bundles gained substantial interest and is continually investigated both numerically and experimentally.

In particular the pressure drop in fuel assemblies represents the thermos-hydraulic property which received the most attention. State of the art practice is to develop correlations for the pressure drop which discriminate between the lumped pressure drop across obstructions such as the spacers and the distributed friction losses in the bare regions of the bundle. Common practice is to experimentally develop these correlations, where a wide variety of data is reported in the literature where various shapes of spacers have been analyzed. To obtain a deeper understanding of flow features CFD studies began to play an increasing role during the last decades. Yet these studies were considered qualitative for a long time. Benchmark studies, e.g. OECD benchmark studies LACANES and MATTIS-H [1-3], performed in the recent years aimed at validation of CFD-studies and accessed precision of different numerical techniques. The experience gained in these studies is that the uncertainty of correlations based on experiments is comparable with the uncertainty of CFD. These benchmark studies demonstrate that the accuracy of results not only depends on the physical models which are used but to substantial extent on the experience of the CFD-user. In this paper we exploit the experience gained in the benchmark studies above for pre and post-test analysis of HLM 19-pin rod-bundle experiments performed at the Karlsruhe Liquid Metal Laboratory (KALLA) of Karlsruhe Institute of Technology (KIT) within the framework of the EU-FP7 project THINS (thermal hydraulics of innovative nuclear systems) [4]. The experiment use lead-bismuth eutectic as working fluid (LBE). The tested experiment aims at supporting the design of bundles for the European ADS Gen-IV reactors. Therefore, it has characteristic dimensions close to the designed ADS European bundles for Gen-IV reactors. The design of the experiment was chosen making use of experience gained from prior water experiments at KALLA. Comprehensive pre and post CFD analysis was performed on these water experiments within the EU FP6 EUROTRANS project, see [5.6].

For the current experiment pretest analysis of various effects such as symmetry and inflow domains were studied. Details of the spacer geometry was selected according to the temporary design proposal at the time of simulation. Since the final experimental campaign used a slightly modified spacer grid we perform in our post-test analysis a last study which exploits all the experience from the pretest studies. The pretests CFD studies as well as the experimental findings and available correlation had shown that the drag coefficient of the spacer is near constant for high Reynolds number. Accordingly a single nominal flow rate was used for posttest numerical investigation. The correlations just relate pressure drop across spacers with blockage ratio and Reynolds number and in addition in a few cases they distinguish weather the leading edge of the spacer is sharp or round even though there are many other effects, which may influence pressure drop. In our posttest analysis we specifically investigate the effect of surface roughness, which usually is not considered in correlations. Moreover, we consider two cases with identical characteristic blocking ratios but exhibit distinct blockage at the leading edge. This can be accomplished with the tested spacer grid which has different blockage ratio at the leading and trailing side. This provides insight to the effect of blockage ratio at the inlet compared to the characteristic blockage of the spacer. These three selected flow cases are formally identical when applying correlations based on pressure loss coefficient and local blockage. Yet these cases differ in roughness and leading-edge blockage ratio.

The structure of this paper is as follows. In section 2 the experiments are described and important parameters are given. A thorough comparison to existing correlations is performed. In section 3 pre and post-test studies are presented. Final conclusions are given in section 4.

2. KALLA LBE Bundle experiment

The test section of THEADES loop of the KALLA-Lab with 19-pin rod bundle experiment is illustrated in Fig. 1. A uniform velocity up stream of the bundle is insured by a suitable design of the upstream flow-conditioning section, where the flow enters the test section through slots arranged peripherally as shown in

Fig. 1. In the experiment the pins are held by a pin fixer downstream of a Venturi nozzle and three spacer grids. This behavior of the flow downstream of the Venturi nozzle was verified in the water experiment conducted within the EU-FP6 EUROTRANS project. Numerical results computed for the velocity distribution show that the flow is homogeneously approaching the pin fixer [5]. The test sections geometrical parameters and operational ranges of are summarized in table I, see [7].

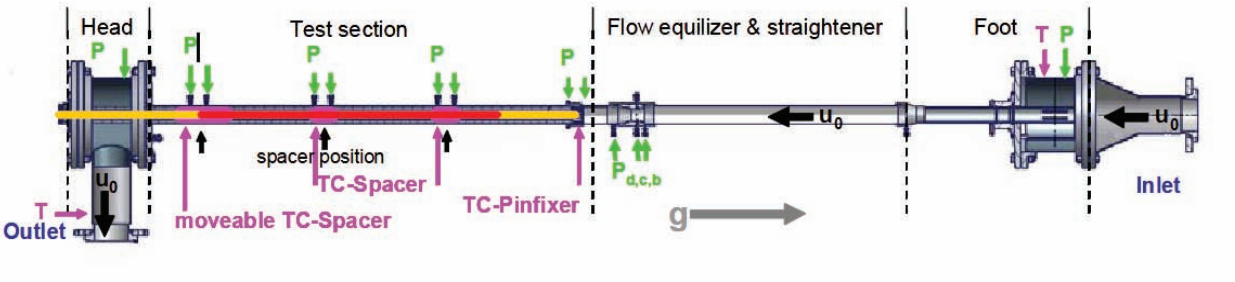

Figure 1 Instrumentation of the LBE rod bundle experiment.

Table I. Geometrical parameters and operational ranges of the test section

geometrical parameter	**value**	**operating range**	**value**
rod diameter (D)	8.2 mm	temperature (T)	200 – 450 °C
pitch-to-diameter ratio (P/D)	1.40	heat flux (Q)	50 – 440 kW
number of rods / spacers	19/3	heat flux density (q_w)	118 – 1033 kW/m^2
heated length of the rods (L)	870 mm	mass flow rate	4.3 – 31.7 kg/s
length of the spacers (L_{sp})	25 mm	Prandtl number (Pr)	0.0147 – 0.0345
hydraulic diameter of a central sub-channel ($d_{h,sch}$)	9.52 mm	Reynolds number	10 200 – 128 000
hydraulic diameter of the bare-bundle flow channel ($d_{h,bdl}$)	7.70 mm	Péclet number	291 – 3600

Details of the final design of the tested spacer are given in Fig. 2 and in [8]. Fig. 2 shows that the spacer has several walls with variable thickness. This became necessary in order to manufacture holes for thermocouples to pass through. As a result, the tested spacer exhibits a blockage ratio of 0.16 at the leading edge (spacer inlet), 0.29 at the spacer mid-plane, and 0.27 at the spacer exit. Here the blockage ratio or solidity (e) is defined as the ratio of the projected spacer grid cross section at a given position to the undisturbed flow cross section in bundle. Commonly the spacer is characterized by its maximum blockage ratio, i.e. in our case e = 0.29. In the previous studies related to water and LBE experiments, spacers with blockage ratio of e =0.27 and e =0.34 were used.

The measured pressure drop at each spacer has two contributions, namely the lumped pressure drop of the spacers (25 mm height) and the distributed friction losses in the bare regions of the bundle (75 mm height) here a distance of 100 mm between pressures measuring probes is considered, see [9]. These are represented in terms of two non-dimensional parameters: K_{sp} and f, defined in Eqs.1-2, respectively.

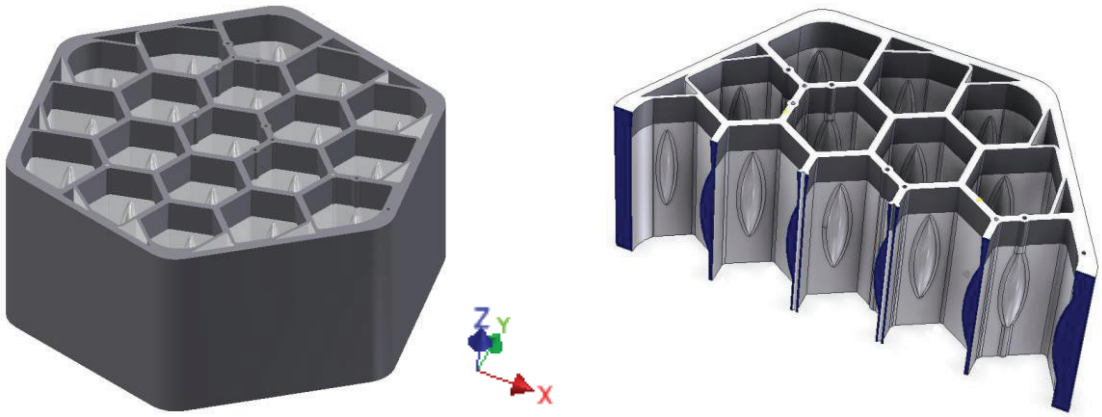

Figure 2. Spacer equipped with installation holes for thermocouples (flow direction in the experiments is in positive z-direction)

$$K_{sp} = \frac{\Delta P_{sp}}{1/2\ \rho u_b^2}, \tag{1}$$

$$f = \frac{\Delta P_f}{1/2\ \rho u_b^2} \frac{d_{h,bdl}}{L}. \tag{2}$$

Accordingly, the pressure drop in the spacer is calculated by subtracting the pressure drop corresponding to the pressure losses in the 75 mm from the measured pressure drop. In this consideration the Darcy friction factor *f* was calculated according to [10]. The calculated value differs just a few percent from the value according to Blasius's equation, (more details can be found in [9]). The experimentalist proposed a correlation for the measured pressure drop of the spacer, which represents the measured values within a range of 10 percent accuracy. The correlation provides a modified loss coefficient c_v as a function of Re as follows:

$$c_v = 1.315 + \frac{9.455}{\mathrm{Re}^{0.407}} + \frac{10.561}{\mathrm{Re}^{0.43}} \tag{3}$$

where the drag coefficient K_{sp} in Eq. 1 can be calculated from c_v and the solidity of the spacer *e* as:

$$K_{sp} = c_v * e^{0.2} \tag{4}$$

In [11] another correlation of similar form was proposed for spacers with sharp edges. They present the following correlation:

$$c_v = 1.104 + \frac{791.8}{\mathrm{Re}^{0.748}} + \frac{3.348\mathrm{x}10^9}{\mathrm{Re}^{5.652}} \tag{5}$$

where K_{sp} is calculated according to Eq. 4. The correlation is recommended to predict spacer losses both for rounded and sharp edges with an expected error of about 15 percent. They also recommended another correlation for spacers with rounded leading edges. The recommended correlation was previously proposed by Cigarini and Dalle Donne in 1988 [12]. This correlation was based on data of Rehme [13]. The correlation reads:

$$c_v = 3.5 + \frac{73.14}{\mathrm{Re}^{0.264}} + \frac{2.79\mathrm{x}10^{10}}{\mathrm{Re}^{2.79}} \quad (6)$$

with

$$K_{sp} = \min(c_v e^2, 2) \quad (7)$$

The above correlations (Eqs. 3, 5 and 6) provide a certain range of accuracy, see [9] and [11-13]. Figure 3 shows a comparison of these correlations as a function of Reynolds number for a spacer with given blockage ratio corresponding to the spacer of Fig. 2, *e*=.29.

According to the correlations rounded leading edge spacers have substantially lower pressure losses compared to spacers with sharp edges. The correlation representing our experiments at KALLA which uses a sharp edged spacer grid is expected to coincide with the correlation of [11], Eq. 5. Yet it delivers higher values than predicted. One of the main objectives of our numerical studies will be to get some insight into this wide variety of prediction. Note that c_v is near constant for high Re so that it suffixes to study a single high Reynolds number case later on.

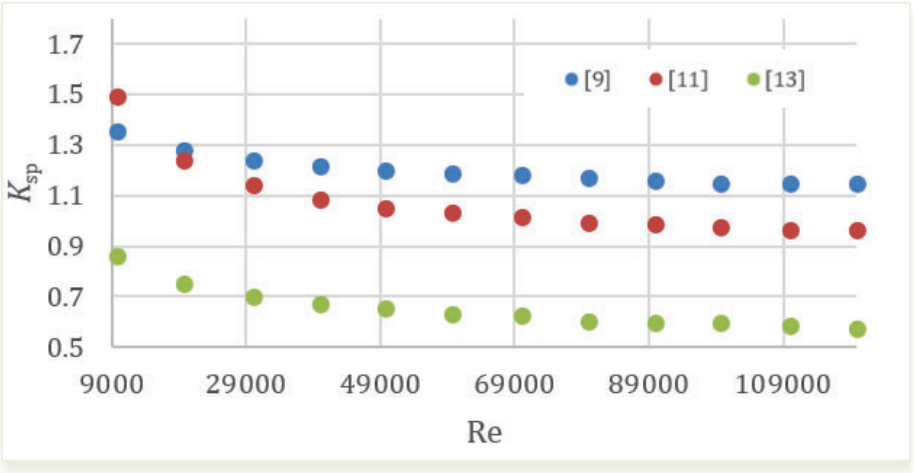

Figure 3 shows a comparison between experimental data of KALLA [9] and correlations of, [11, 13]

3. Numerical study

Our pretest studies within EU-FP7 THINS project show that the computed pressure drop when accounting for the exact spacer geometry is less than the measured pressure drop. Accordingly other factors were discussed, including roughness. It could be shown that roughness is an important factor which increases the pressure drop, consequently decrease the difference between experimental and numerical results. The roughness of the tested spacer is 35-40 μm whereas the heated rods are considered smooth. For the present posttest study it is decided to consider the roughness in the spacer as well as the exact geometry which is tested in the experiment. This will enable quantitative comparison between numerical and experimental results.

The correlations in Eqs.3-7 relate the pressure drop to the blockage ratio independent of how the blockage is formed. In particular, the tested spacer in figure 2 is characterized by a maximum blockage located in center plane. As discussed above, inlet and outlet blockage can differ for various spacer designs exhibiting identical characteristic blockage ratio. Reversing the flow direction for our spacer (see Fig. 2) we may explore the uncertainties related to the how the blockage is formed without the need to study a spacer with a new geometry. In the experiment the flow enters the spacer subject to a sudden blockage ratio of 0.16, i.e. corresponding to a sharp edge. Downstream the flow accelerates until the blockage ration of 0.29 is reached in the center plane decelerates following the dimples and slightly accelerates towards the exit where the blockage ratio becomes 0.27. In the reversed case the flow passes a strong sudden blockage of 0.27 blockage at the leading edge and then slightly decelerates as it approaches the dimples where it has to accelerate again. Downstream of the dimples the flow decelerates substantially until it exits at the location of minimal blockage ration. In particular both cases differ by the fact that at the leading edge substantially different blockage is observed. Since the correlations for sharp and round edged leading edges indicate sensitivity of pressure drop on the leading edge we expect the case of reverse flow with the more pronounced blockage to exhibit larger pressure drop.

The present study is carried out for the nominal mass flow rate of 26 kg/s. The experimentally measured average pressure drop for this nominal case is 27.5 kPa ±7%. The uncertainty is deduced from the variations between the measurements of the three successive spacers and also some variations of temperature during the experimental campaigns. The measured pressure drop represents the pressure drop between pressure measuring probes located 100 mm apart. Considering that the spacer length is 25 mm, the measured pressure drop accounts for the spacer and additional 75 mm part of the bare bundle. The experimental data represented by Eq. 3 results in 23.8 kPa for the spacer pressure drop at Re=88 10^3 (nominal flow rate). For the bare rod region of 75 mm length, a pressure drop of 3.7 kPa as described above. Note that the predicted pressure drop in the bare rod region and the pressure drop according to the Blasius equation are almost identical. Before we discuss the studied cases in details we review most important results of the pretest analysis.

3.1 Pre-test analysis for KALLA experiment

The pretest studies to support the design of the experimental test section including the flow straightener are reviewed in this section. As described above the experiment is designed exploiting results obtained from the previous water experimental and many other numerical studies. In [14], studying the water experiment, different flow domains and meshes were considered. The studied computational domains in [14] are shown in Fig. 4. The figure depicts the tested domains include one or two spacers, simulated spacer, sample mesh in a plane cutting the spacer and the surface mesh on selected boundaries. The characteristic blockage in the pre-test simulations was e= 0.27. The pre-test study demonstrates that the pressure drop across the first and second spacer grid are nearly identical. Moreover, the pressure gradient in the inlet section and the section downstream of the spacers is near identical, so that development effects can be ignored. Accordingly, it was recommended that in future simulations it suffices to analyse a single spacer grid with cyclic boundary conditions. The mesh refinement study in [14] shows that the mesh in the spacer region must be refined substantially in order to achieve mesh independent solutions. In another study [15] considering also the water experiment, the effect of the pin fixer and the region upstream of the test section were investigated by considering a flow domain including the first spacer and the flow equalizer region. The study also investigated the working assumption of substantially enhanced pressure drop for the first spacers compared to the other spacers as a consequence of substantial flow concentration downstream of the Venturi nozzle. The study has shown that the upstream region does not affect the pressure drop in the first spacer where similar pressure drop was observed as that obtained from flow domains shown in Fig. 4. In addition [15] compared pressure drop measured and computed to the literature. In the comparison a correlation from [12] which correlate the experiment results of [13] was selected. The comparison shows that the tested spacer results in a relatively higher pressure drop values than that predicted by the correlation.

In the above comparison a quit good agreement between CFD pressure drop results and measured results was observed for low and high Reynolds numbers.

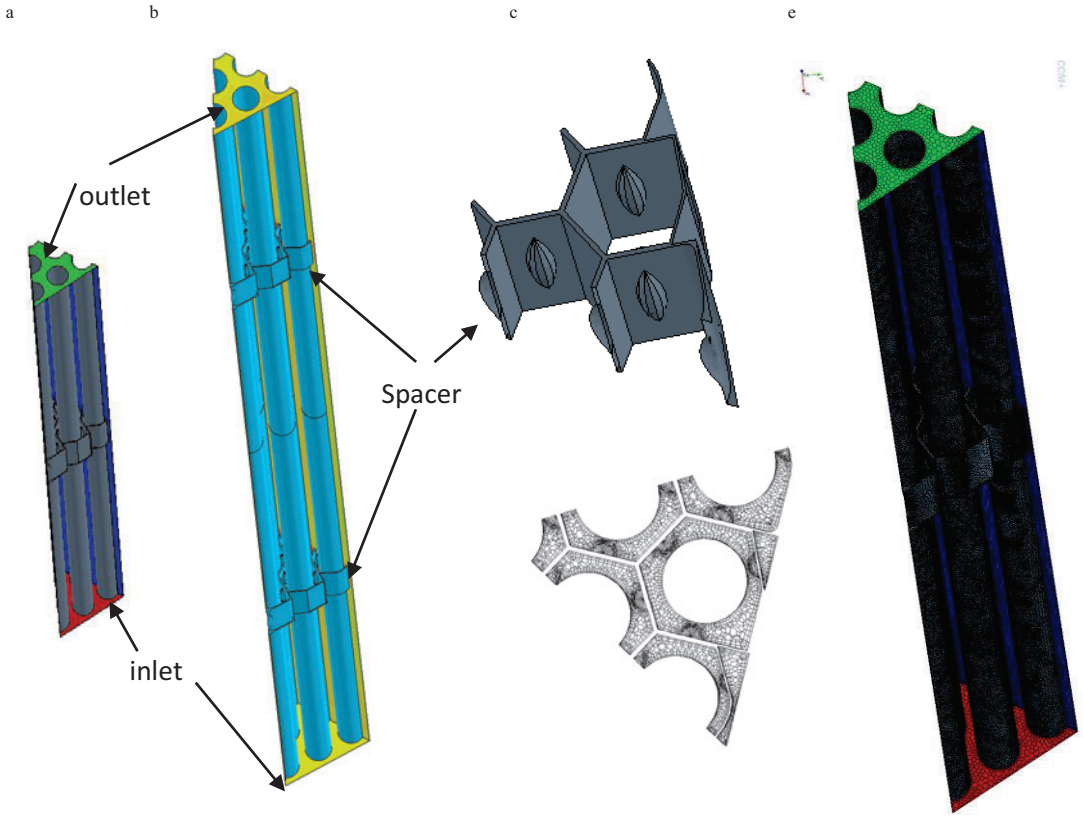

Figure 4 **Computational domain with a) one spacer. b) with two spacers, c) spacer geometry, d) mesh in a plane cutting spacer, e) surface mesh at selected boundaries**

For the pretest study for the LBE experiment a similar type spacer as used as for the water experiment, see [16]. However, it considered blockage ratio *e*= 0.34. Based on the previous results of [14,15] the simulation considered in [16] were restricted to the entrance region including one spacer. As explained above for the first test two computational domains were used. The first includes all details of geometry in the bundle upstream by including Venturi nozzle and pin fixer etc. The other domain is simplified and covers only a sector of 60° similar to shown in Fig. 4-a. A domain covering a 360° sector is meshed with approximately 2 million cells while a domain corresponding to a 60° sector is meshed with 0.2 million cell. The standard k-ε model with high y+ wall treatment is used. Unsteady computations are performed leading to a steady state solution for the nominal mass flow rate of 26 kg/s. The study of the two different domains with uniform inflow have demonstrated that the selected smallest computational domain which exploits all possible symmetries already delivers comparable results to the full domain computation. This highlights the very weak effect of the entrance region on the computed pressure drop across the spacer. Moreover [16] conducted a sensitivity study using different meshes and different models and shows that the mesh effect is more pronounced than the effect of the tested wall treatment and turbulence models. This indicates that complex effects such as flow recirculation which require specialized turbulence models are not very pronounced in the considered bundle geometry.

3.2 Post-test analysis

The post-test analysis of the experiment consider a sector of the bundle which include one spacer. We also consider a 60º sector as in the previous studies. Due to the 120° symmetry of the new spacer we also use the smallest sector possible which corresponds to a 120º sector of the bundle. A mesh of 1.65 million cell was generated for this simulation. The simulations employ the Star-CCM+ code, high-Reynolds-number k-ε-turbulence model with automatic wall treatment. In the experiment the heated rods are considered smooth. However, the spacer exhibits a surface roughness of 35-40 μm. Accordingly, the mesh is generated so that the first wall distance is kept in the range of the spacer roughness. In case of the rough wall boundary condition, the code picks the minimum of the specified roughness wall or the wall distance. Fig. 5 shows the wall distance of the first cell centroid to the wall in our posttest simulation.

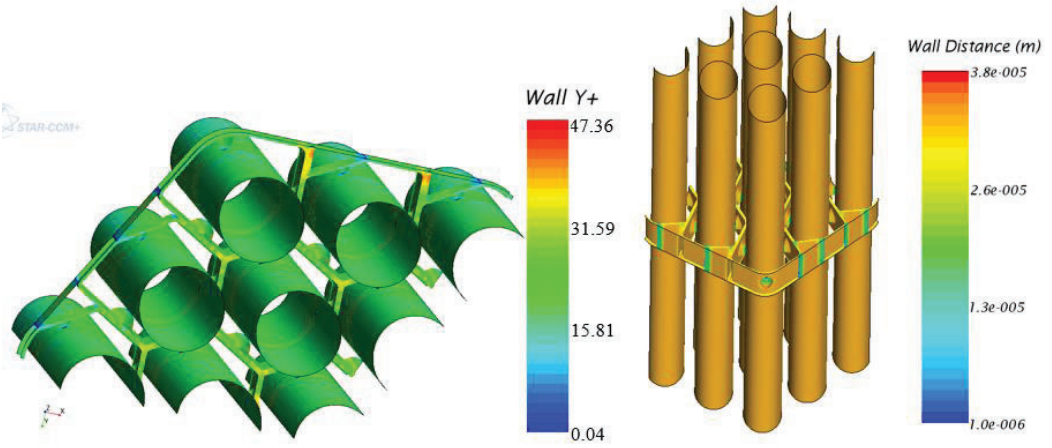

Figure 5 **Contours of the y^+ and wall distance**

The study is carried out for the nominal mass flow rate of 26 kg/s with uniform inlet velocity and constant fluid temperature, T=300C°. This corresponds to volumetric flow rate of 9.1 m^3/h. This flow rate was also consider in the previous studies [16]. For consistence and further comparisons it is maintained here. Experimental results are available for a range of flow rate, 1-11.5 m^3/h. A nearly constant pressure loss coefficient is obtained for a wide range around the nominal case. The experimentally measured pressure drop for our nominal case is 27.5 kPa ±7%. Three cases will be presented in the post test study. In the first case (i) the condition of the experiment with rough spacer and smooth rods is considered. In the second case (ii) identical conditions ignoring roughness are considered in order to evaluate the effect of roughness. In these cases (i and ii) the orientation of the spacer (shown in Fig. 2) with flow in the +z direction is considered, which also corresponds to the flow direction of the experiments. In a third case (iii) the conditions of case (ii) is considered by reversing the flow direction. This enables us to check the validity of relating the pressure drop coefficient to the characteristic blockage ratio of the spacer but ignoring the local blockage at the leading edge. In case (iii) the spacer has blockage ratio of 0.27 at spacer leading edge, 0.29 at spacer middle plain and 0.16 at the trailing edge.

Fig. 6 shows the pressure drop along selected lines across the spacer. In the experiment probes where installed 5cm upstream and downstream of the spacer middle plane, i.e. at a distance of 10 cm. The planes in the figure are exactly positioned at the measurement positions. The pressure drop is calculated based on the difference between the area average pressures up and down stream of the spacers as shown in the figure by pressure contours. Accordingly, the pressure losses in the spacer including 10 cm is about 25.0 kPa. The

calculated pressure profile also shows the axial pressure gradient of 55 kPa/m which corresponds to frictional losses of 4.1 kPa in the bare rod region of 7.5 cm length. The calculated pressure gradient is determined sufficiently far from the spacer where the pressure profile behaves linear. This value can be compared to predictions based on the Blasius equation for pressure drop and [10], which both result in approximately 3.7 kPa.

Fig. 7 shows a comparison of the cases (ii) and (iii). In both cases a smooth spacer with negligible roughness is considered. The flow direction is revered for case (iii). We observe for the smooth spacer in forward direction, i.e. case (ii) has approximately 23.0 kPa between the measurement probes. Remember that this value is area averaged computed pressure 5 cm upstream and downstream of the spacer middle plane. The additional effect of roughness can be deduced from the difference of cases (i) and (ii) and accumulates to just 2 kPa. Reversing the flow direction we compute at the same probe positions a higher pressure drop of 26.3 kPa. The additional pressure is attributed to the higher leading edge blockage e=0.27 of the spacer in reverse direction, i.e. case (iii) compared to the leading edge blockage e=0.16 in forward direction, i.e. case (ii). Since cases (i-iii) all have the same spacer geometry, i.e. blockage ratio and the same Reynolds number they should have the same pressure loss according to above presented correlations. Yet there is a substantial difference, which highlights the importance of leading edge blockage and roughness.

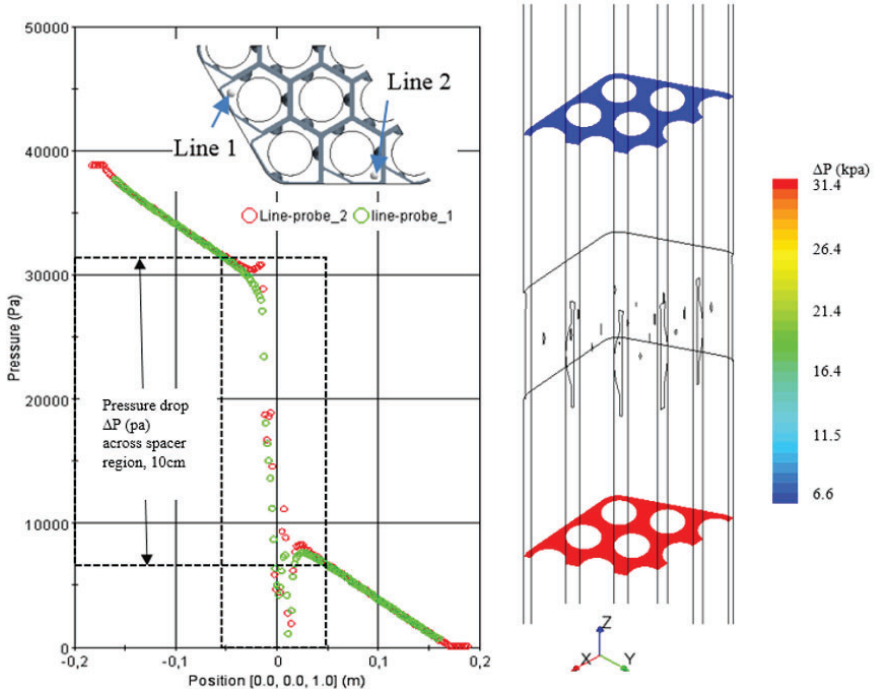

Figure 6 Pressure drop along selected lines across the spacer and pressure contours 5 cm upstream and downstream of spacer middle plane, case (i)

Table II summarizes and compares the resulting pressure drop across the spacers for the considered cases. The comparison between numerical and experimental results shows that the numerically predicted pressure is 10% less than measured. Better accuracy was observed in the pre-test studies where spacers with blockage ratio of 0.27 (water experiments) were considered [14,15]. According to previous experience we speculate that the remaining small difference, within the accuracy bounds of the measurements, between numerical and experimental values could indicate some additional blockage in the spacer due to crude. This finding is supported by the fact, that the experimentally measured pressure drop across a spacer is always lower

compared to its successive spacer, even though the opposite effect is expected due to the developing flow conditions. The comparison of cases (ii) and (iii) shows the pronounced effect of leading edge blockage on the pressure drop in the spacer. Note that both cases correspond to the classification of a sharp edge according to [11]. Thus in addition to the shape of the leading edge, correlations should also consider leading edge blockage and possibly further parameters like the length of the spacer as well as the profile of blockage along the length.

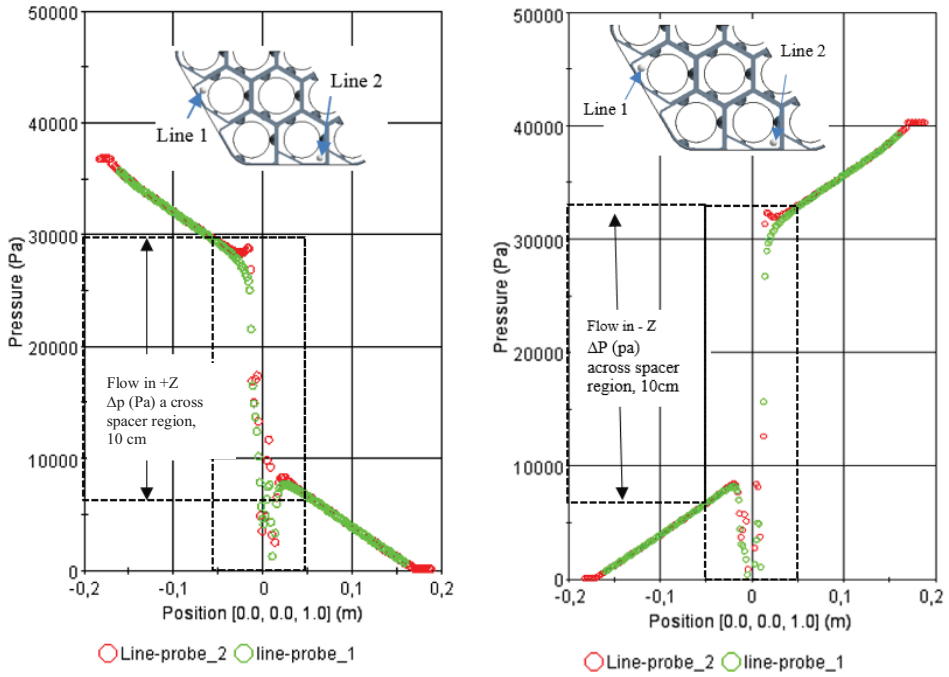

Figure 7 Pressure drop along selected lines across the spacer (no surface roughness); left side forward flow direction similar to experiment, case (ii); right side reversed flow, case (iii)

Since CFD is capable to distinguish all these factors and many more within the uncertainty range of the experimental date it can be recommended for the prediction of spacer pressure losses. Moreover, CFD is very well suited to explore the trend when making variations in design. It should be noted that the available correlation are based on limited data points and specific spacer geometry. Therefore the actual uncertainty when applying correlations for a brand new spacer geometry is quiet large. Therefore we recommend to develop a new spacer design by first applying correlations for a rough estimation, then applying CFD for the detailed design work, and finally by verifying the final design based on experiments.

Table II. Comparison of pressure losses for considered cases

	experimental	**rough spacer, case (i)**	**smooth spacer, case (ii)**	**smooth spacer reversed, case (iii)**
Δp (kPa)	27.5±7%	25.0	23.0	26.3
roughness error in %	reference (27,5 kPa)	-10%	-16.4	-
flow direction effect error in %	-	-	reference (23 kPa)	+14.3%

Conclusions

Our investigation of pressure loss in rod-bundle geometries with spacer grids explored an experiment which was performed at KALLA and used liquid metal as fluid. CFD has shown to reproduce the measured date within the range of uncertainty of the experiment. The state of the art procedure when designing new spacers is to apply correlations. We found numerous correlations applicable to the same design, which mainly depend on Reynolds number and blockage ratio. One correlation accounted for the shape of the leading edge, by distinguishing round and sharp. CFD can be performed using the actual geometry of the spacer including all its geometrical features and thus can be used to study these effects in much detail. Specifically we studied three cases which are all equivalent according to the correlations and yet show substantial difference in their pressure losses, e.g. roughness accounted for 6 % and leading edge effect for 14%.

In the presented pretest studies we applied a systematic scheme which leads to accurate predictions. This begins by selecting a suitable domain, mesh and turbulence model. For parametric studies we use the smallest representative geometry with a well resolved numerical mesh concentrated in the spacer region. The obtained difference between post-test numerical and experimental values shows that CFD can be recommended for the prediction of pressure loss in spacer with equivalent accuracy as found in the experiment.

ACKNOWLEDGMENTS

This work has been supported by FP7 Thermal-Hydraulics of Innovative Nuclear Systems (THINS), Grant 249337 and the AREVA nuclear professional school.

REFERENCES

1. J. Cho, et. al., Benchmarking of thermal hydraulic loop models for Lead-Alloy Cooled Advanced Nuclear Energy System (LACANES), phase-I: Isothermal steady state forced convection , Journal of Nuclear Materials 08/2011; 415(3):404-414
2. A. Batta, et. al., CFD analysis of heavy liquid metal flow in the core of the HELIOS loop, Nuclear Engineering and Technology 12/2010; 42(6).
3. A. Batta, CFD study of isothermal water flow in rod bundle with split-type spacer grid. SNA & MC 2013, Paris; 10/2013
4. Annex I – "Description of Work for THINS project", Seventh framework programme of EURATOM for nuclear research and training activities (2007-2011), theme: nuclear fission and radiation protection , grant agreement for: Collaborative project "large-scale integrating project, no.: 249337
5. Annex I, EUROpean Research Programme for the TRANSmutation of High Level Nuclear Waste in an Accelerator Driven System, Project acronym: EUROTRANS, Contract no.: FI6W-CT-2004-516520, Feb. 2005
6. K. Litfin, "EUROpean Research Programme for the TRANSmutation of High Level Nuclear Waste in an Accelerator Driven System", FI6W-CT2004-516520, Workpackage N°: W 4.5, .Identification N°: D 4.68
7. J. Pacio, et. al., Heat transfer to liquid metals in a hexagonal rod bundle with grid spacers: Experimental and simulation results, Nuclear Engineering and Design (2014), In Press, Corrected Proof,
8. J. Pacio, et. al., Mid-term report on experimental rod bundle data, Technical Report, THINS Deliverable 1.1.06,2013
9. J. Pacio, et. al.,. Heavy-liquid metal heat transfer experiment in a 19-rod bundlewith grid spacers. Nucl. Eng. Des. 2014, 273, 33–46.

10. Cheng, S.-K., Todreas, N.E., 1986. Hydrodynamic models and correlations for bareand wire-wrapped hexagonal rod bundles – bundle friction factors, subchannelfriction factors and mixing parameters. Nucl. Eng. Des. 92 (2), 227–251.
11. Epiney, A., Mikityuk, K., Chawla, R., 2010. TRACE qualification via analysis of the EIRgas-loop experiments with smooth rods. Ann. Nucl. Energy 37 (6), 875–887.
12. M.Cigarini, M.Dalle Donne, "Thermohydraulic optimization of homogeneous and heterogeneous advanced pressurized reactors", Nuclear Technology, Vol.80, pp.107-132 (1988).
13. K. Rehme, Pressure drop correlations for fuel element spacers, Nuclear Tech., 17, pp. 15-23, 1973
14. A. Batta, A. Class, K. Litfin, T. Wetzel "Numerical Study on Flow Distribution and Turbulent Flow in XT-ADS Rod Bundle Water Experiment", NUTHOS-8, paper N8P0232, Shanghai, China, Oct 10-14, 2010
15. A. Batta, A. et. al., Rehme Correlation for Spacer Pressure Drop Compared to XT-ADS Rod Bundle Simulations and Water Experiment, JTK 2011
16. A. Batta, A. G. Class Study of enhanced entrance pressure losses in a rod bundle experiment employing heavy liquid metal coolant, NURETH-14 Toronto, Ontario, Canada, 2011